

Brownian Motion Delay Model for the Integration of Multiple Traffic Management Initiatives

Juan Rebollo and Chris Brinton

Mosaic ATM, Inc.
Leesburg, VA, USA

jrebollo@mosaicatm.com, brinton@mosaicatm.com

Abstract—There is no technology that provides effective support for procedural consideration of the effect of strategic programs on tactical Traffic Management Initiatives (TMIs) and vice versa. A key challenge in the design and use of Air Traffic Management (ATM) decision support tools is to determine how much control should be applied to the flow of traffic and at what point in the flow should it be applied. This challenge has significant impact on the resulting effectiveness of any ATM control program that is applied, because inefficiencies can be caused by either under or over-control of the flow. This paper presents a new analytical approach based on a Brownian Motion (BM) formulation, which quantifies the interactions between TMIs. The proposed General Brownian Motion (GBM) model takes as input uncertain and dynamic demand and capacity and provides an estimate of the delay distribution associated with the TMI controlling the demand. The obtained delay distribution can be used to estimate the probability of over-controlling or under-controlling the flow for the selected TMI parameters. Interactions between TMIs can be characterized by evaluating the probability that one TMI over-/under-controls the flow seen by a down-stream TMI. The delay prediction performance of the model is evaluated using actual Time-Based Flow Management (TBFM) data for PHL, and three case studies including multiple days of data are presented to demonstrate operational uses of the GBM model over two different TMIs and three airports.

Keywords-TMIs interaction; demand/capacity uncertainty; stochastic analytical approach; Brownian Motion; delay modeling

I. INTRODUCTION

An integrated decision support capability is needed to provide Air Traffic Management (ATM) specialists and flight operators with information to support planning and decision-making about tactical and strategic Traffic Management Initiatives (TMIs). The significant challenge that exists in providing this capability is the uncertainty of prediction of both demand and capacity. This paper addresses this shortfall by presenting an innovative analytical approach, which uses a Brownian Motion (BM) [1] formulation to translate uncertain demand and capacity into a delay distribution.

There are a number of key aspects of any traffic flow situation that drive the appropriateness of any particular TMI that could be used. The aspects include:

- The efficiency of the impact of the TMI (i.e., is there any excess delay?)
- The equity of the effects of the TMI across flights, flight operators, geographical regions, etc.

- The temporal range of the impact of the TMI (i.e., strategic or tactical)
- The uncertainty of demand and capacity predictions

The ideal solution to these computational problems would be the identification of a closed-form stochastic (i.e. including demand and capacity uncertainty) analytical solution that could be used to evaluate TMIs, without the need of running a Monte Carlo simulation. Our focus in this research effort is on the formulation and application of an analytical approach to modeling the impact of individual TMIs and the modeling of interactions between TMIs.

Significant work has been done previously on related issues. For example, Grabbe [2] performed a detailed study of the use of a Ground Delay Program (GDP) procedure intended to coordinate the strategic GDP with the more tactical use of Traffic Management Advisor (TMA, now called TBFM) time-based metering and associated internal departure scheduling. Grabbe's work identified the complexity of matching the tactical and strategic delay through the use of 'coordinated' strategic and tactical flow management techniques. Recent work has been performed by Wanke [3] addressing the interrelated impacts of multiple TMIs, and means to compute and visualize the decision space for Traffic Management Coordinators (TMCs). Wanke's work utilizes a simulation approach in which individual fast-time simulations are performed of each of a discretized set of points in the search space of possible TMI combinations. They explored combinations of: one GDP, one AFP, and two re-route advisories in the Atlanta Center (ZTL).

The research community has developed a wide range of models to evaluate the effects of demand and capacity uncertainty on traffic flow. Queuing models capturing demand uncertainty were proposed in [4-6]. Yan and Roy's work [7-8] introduce a saturation model and the use of Markov-chain models to facilitate the systematic analysis of queue's transient dynamics. Uncertainty has also been addressed by using multiple scenarios in [9, 10], where capacity uncertainty is modeled by considering the most likely scenarios.

The proposed General Brownian Motion (GBM) delay model differs from the above models by providing a closed-form stochastic analytical solution, and including both uncertain and dynamic demand and capacity. A key aspect of our model is that its output is a delay distribution, which allows us to easily obtain the probability of over-control (wasted capacity)

or under-control (excessive delay) of the flow. It is also important to highlight that the delay distribution is calculated in a short computational time thanks to the analytical formulation.

A stochastic analytical solution to the characterization of the impact of TMIs on traffic flow and delays is a significant advancement in the state-of-the-art in traffic flow modeling and analysis, and could accelerate the successful development of a decision support tool that can provide NAS-wide system impact assessment.

The remainder of the paper is organized as follows. Section II describes the GBM model formulation. Section III evaluates the performance of the model in its accuracy of prediction of both the delay and the true distribution of the delay. Section IV demonstrates operational uses of the GBM model through three case studies. Section V closes the paper with conclusions and next steps.

II. BROWNIAN MOTION DELAY MODEL

A. Introduction

This section introduces the BM delay model assuming constant demand with uncertainty and constant capacity without uncertainty. Subsequent sections will expand the model equations for varying demand and capacity, and uncertainty in both demand and capacity.

The delay at a resource, $\hat{Y}(t)$, can be model as a function of demand, $\hat{D}(t)$, and capacity, $\hat{C}(t)$, as follows:

$$\hat{Y}(t) = \int_0^t \frac{\hat{D}(t) - \hat{C}(t)}{\hat{C}(t)} dt \quad (1)$$

Assuming that there is uncertainty only in the demand and both demand and capacity are constant, we can write: $\hat{D}(t) = D + \epsilon(t)$ and $\hat{C}(t) = C$, where $\epsilon(t)$ is the demand error or uncertainty term, and we can rewrite equation (1) as follows:

$$\begin{aligned} \hat{Y}(t) &= \int_0^t \frac{D + \epsilon(t) - C}{C} dt \\ &= Y_0 + \frac{D-C}{C}t + \frac{1}{C} \int_0^t \epsilon(t) dt \end{aligned} \quad (2)$$

As such, the delay as a function of time consists of three components: some initial delay, Y_0 , a component that grows linearly in time, $\frac{D-C}{C}$, and a component involving the integration of the demand error term, $\epsilon(t)$. If we assume that this demand error is a zero-mean, Gaussian random variable, we can compute a closed-form form for $\hat{Y}(t)$:

$$\hat{Y}(t) = Y_0 + \frac{D-C}{C}t + \frac{\sigma}{C}W(t) \quad (3)$$

where $W(t)$ is the standard BM process generated by the integration of the Gaussian error term, and $\hat{Y}(t)$ is a BM process with drift [1, 10]. Consequently, the PDF of $\hat{Y}(t)$ is given by:

$$PDF_Y(t, y) = \frac{1}{\frac{\sigma}{C}\sqrt{2\pi t}} e^{-\frac{(y-Y_0 - \frac{D-C}{C}t)^2}{2(\frac{\sigma}{C})^2 t}} \quad (4)$$

The approach uses the statistical characteristics of delay as computed using (4) to determine the probability of under-control and of over-control of the flow. The probability of over-control of the flow is represented by the portion of the PDF that is less than zero, indicating that negative delay would need to be applied to the flow to utilize the full available capacity:

$$P(\text{over-control})(t) = \int_{-\infty}^0 PDF_Y(t, y) dy \quad (5)$$

And the probability of under-control is modeled as the probability that the delay on the flow will exceed some threshold delay, Y_T :

$$P(\text{under-control})(t) = \int_{Y_T}^{\infty} PDF_Y(t, y) dy \quad (6)$$

B. Time-Varying Demand and Capacity

We model time-varying demand and capacity as a piece-wise constant function. At each step both demand and capacity are modeled as normal random variables:

$$D(t), \epsilon_D(t), C(t), \epsilon_C(t) = \begin{cases} D_0, \epsilon_{D_0}, C_0, \epsilon_{C_0} & : t_0 \leq t < t_1 \\ D_1, \epsilon_{D_1}, C_1, \epsilon_{C_1} & : t_1 \leq t < t_2 \\ \dots & \\ D_{N-1}, \epsilon_{D_{N-1}}, C_{N-1}, \epsilon_{C_{N-1}} & : t_{N-1} \leq t < t_N \end{cases} \quad (7)$$

where $\epsilon_{D_i} \sim N(0, \sigma_{D_i}^2)$ and $\epsilon_{C_i} \sim N(0, \sigma_{C_i}^2)$. This formulation allows us to decompose the integral in (1) and we will be able to write $\hat{Y}(t)$ as a sum of integrals with constant terms. See the next section for details. The normal approximation of demand and capacity uncertainty was validated in the error analysis presented in Section III.

C. General Brownian Motion Delay Model

In this section we present the general formulation of the BM delay model, which we denote as the GBM model. The GBM model includes time-varying and uncertain demand and capacity, defined as a piece-wise constant functions as shown in (7). For $t_k \leq t < t_{k+1}$, we can rewrite (1) as follows:

$$\begin{aligned} \hat{Y}(t) &= \int_0^t \frac{D(t) + \epsilon_D(t) - (C(t) + \epsilon_C(t))}{C(t) + \epsilon_C(t)} dt \\ &= \int_0^t \frac{D(t) + \epsilon_D(t)}{C(t) + \epsilon_C(t)} dt - t \\ &= \int_0^{t_1} \frac{D_0 + \epsilon_{D_0}}{C_0 + \epsilon_{C_0}} dt \\ &\quad + \int_{t_1}^{t_2} \frac{D_1 + \epsilon_{D_1}}{C_1 + \epsilon_{C_1}} dt + \dots + \int_{t_k}^t \frac{D_k + \epsilon_{D_k}}{C_k + \epsilon_{C_k}} dt - t \end{aligned} \quad (8)$$

In (8) the integral is decomposed in sub-integrals where the different parameters are constant. The distribution of the terms $\frac{D_i + \epsilon_{D_i}}{C_i + \epsilon_{C_i}}$ is approximated by a Gaussian distribution using a second order Taylor approximation (TT2) [12]. This approximation leads to the integral of normally distributed

variables in (8), which allow us to model $\hat{Y}(t)$ as a BM process. See Section II.D for details about the TT2 approximation. The approximated distribution of $\frac{D_i + \epsilon_{D_i}}{C_i + \epsilon_{C_i}}$ is given by $N(\mu_{T_i}, \sigma_{T_i}^2)$ with:

$$\begin{aligned} \mu_{T_i} &= \frac{D_i}{C_i} + \frac{D_i \sigma_{C_i}^2}{C_i^3} \\ \sigma_{T_i}^2 &= \frac{\sigma_{D_i}^2}{C_i^2} + \frac{\sigma_{C_i}^2 D_i^2}{C_i^4} + \frac{2\sigma_{C_i}^4 D_i^4}{C_i^6} \end{aligned} \quad (9)$$

The approximated distribution of each of the terms $\int_{t_i}^{t_{i+1}} \frac{D_i + \epsilon_{D_i}}{C_i + \epsilon_{C_i}} dt$ is a BM process with drift and distribution: $N(\mu_{T_i}(t_{i+1} - t_i), \sigma_{T_i}^2(t_{i+1} - t_i))$. By applying the additive property of the Gaussian distribution for independent normal distributions ($N(\mu_1, \sigma_1^2) + N(\mu_2, \sigma_2^2) \sim N(\mu_1 + \mu_2, \sigma_1^2 + \sigma_2^2)$), and including the term $-t$ present in (8) in the mean of the BM process, we have that the approximated distribution of $\hat{Y}(t)$ is the following BM process:

$$\begin{aligned} \hat{Y}(t) &= Y_0 + \mu(t) + \sigma(t)W(t) \\ \mu(t) &= \sum_{i=1}^k \mu_{T_{i-1}}(t_i - t_{i-1}) + \mu_{T_k}(t - t_k) - t \\ \sigma^2(t) &= \sum_{i=1}^k \sigma_{T_{i-1}}^2(t_i - t_{i-1}) + \sigma_{T_k}^2(t - t_k) \end{aligned} \quad (10)$$

$t_k \leq t < t_{k+1}$

D. Taylor Approximation Error Analysis

We are interested in evaluating the effect of the Taylor approximation on $\hat{Y}(t)$. Figure 1 compares the approximated Gaussian (blue) and the empirical distribution (red) of the integral of the nonlinear term $\frac{D_i + \epsilon_{D_i}}{C_i + \epsilon_{C_i}}$. The empirical distribution was obtained using the trapezoidal approximation of the integral and different number of integration steps, $N = 2, 3, 5, 10$ (step size = 1). The approximated Gaussian follows the empirical distribution, and the difference between the distributions decrease as N increases.

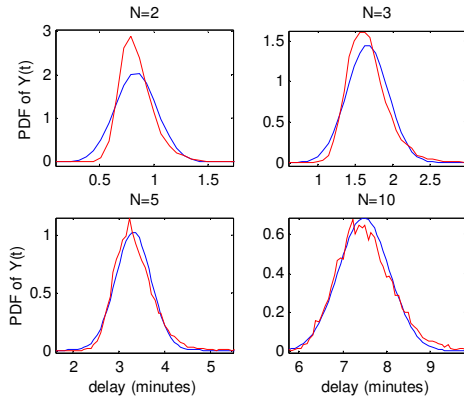


Figure 1. Taylor Approximation Error, empirical distribution in red, Gaussian approximation in blue. $D = 40$, $C = 50$, $\sigma_c = 10$, $\sigma_D = 5$

In this example $\frac{\sigma_c}{C} = 0.2$. Larger approximation errors were identified for large σ_c/C ratios (i.e. >0.4). However, σ_c

denotes capacity uncertainty in both directions, and in our problem it is unlikely that a large change in the capacity value is likely in both directions. For this reason the Gaussian approximation is a valid approximation for our problem.

E. Regulated Brownian Motion

We are modeling the distribution of $\hat{Y}(t)$ as a BM process. A BM process can take any positive or negative value. However, we are not interested in modeling negative delays. Negative delay accumulation represents "stored" capacity that can be used in the future. In reality in the Air Traffic Control (ATC) environment, flights would have to be accelerated to a speed beyond their performance envelope in order to take advantage of this available capacity. In practice, negative delay does not occur with any degree of significance, and thus, negative delay in the GBM model indicates that capacity is actually being lost. However, this loss of the available capacity is not properly represented by the BM model alone.

The Regulated Brownian Motion (RBM) [1] is a BM process with boundaries. The cumulative distribution function (CDF) of a RBM process bounded below zero is given by:

$$P(Z \leq z) = \phi\left(\frac{z - \mu t}{\sigma t^{1/2}}\right) - e^{(-2\mu z/\sigma^2)} \phi\left(\frac{-z - \mu t}{\sigma t^{1/2}}\right) \quad (11)$$

with $\mu \geq 0$. By modeling $\hat{Y}(t)$ as a RBM we would ensure that $\hat{Y}(t)$ is always greater or equal to zero. However, for a RBM process the probability of over-control is always zero, since there is no probability density for negative delay values. For this reason, in the GBM model the probability of over-control is evaluated for a BM process with the mean truncated at zero below. This leads to a maximum over-control value of 0.5 because only at most half of the Gaussian distribution can be below zero since the mean is forced to remain at or above zero.

Even though it is not appropriate to assume that capacity can be stored in the GBM model, and thus negative delay is disallowed, the degree to which the delay in the BM model would go negative is a measure of the true amount of over-control that is predicted. Future research will address methods to include this consideration in the calculation of the over-control probability without allowing future traffic the ability to use the stored capacity. For the remainder of this paper, to avoid confusion and to facilitate the comparison between over-/under-control probabilities, the over-control probability is multiplied by a factor of 2.

III. EMPIRICAL IDENTIFICATION OF PREDICTION ERRORS

This section presents an analysis of the delay prediction error of the GBM model. Note that the GBM model is used to predict both the delay and the distribution of the delay. Thus, our analysis of the accuracy of the model addresses both the mean delay predicted as well as the predicted distribution of the delay. The results were obtained using data from the TBFM system for PHL, and actual delay from surface data. The next three subsections describe the capacity and demand parameters used in the error analysis. The remainder of this

section then presents a detailed evaluation of the GBM model performance.

A. Arrival Capacity Estimation (PHL)

The GBM model approximates capacity as normally distributed variables. We empirically identified the parameters (μ , σ) for the PHL arrival capacity distribution, differentiating between West and East configuration.

We collected 15-minute arrival counts for 5 months of 2014 data (April, May, August, September and October). The arrival rates were obtained by processing actual arrival times from ASDE-X data. We selected 15-minute time intervals in which PHL was operating at full capacity, defined as time intervals where demand exceeds capacity. Demand was obtained using the ETAs available 50 minutes before the actual arrival times.

For the selected time intervals the mean of the distribution for West configuration was 14.5, and the standard deviation was 2.5. If we translate the 15-minute rates to 1-hour rates we have that the interval $[\mu - \sigma, \mu + \sigma]$ is given by [50.7, 60.7]. These values are consistent with the arrival rates published in the Operational Information System (OIS) website¹ for PHL. In West configuration, the preferred arrival rate is 60 fl/h (VMC, arrivals on 27R/35/26), and the wind or fleet mix affected rate is 52 fl/h (VMC).

B. Demand Estimation - From ETA to Demand Distribution

In ATM systems, demand estimation is often generated through a deterministic count of ETAs in an interval. However, the GBM delay model requires a distribution of demand. In this section we solve the following problem: Given a set of flights with an assumed arrival time distribution, find the equivalent count distribution within a given time interval, denoted by $[t_s, t_e]$. This is a necessary step to run the GBM delay model, since it provides the terms D_i and ϵ_{D_i} in (7) which are obtained as the counts distribution in the $t_i \leq t < t_{i+1}$ time intervals.

Monte Carlo simulations in [13] showed evidence that trajectory control time errors follow a bell-shape distribution. We assume that the time of arrival for a given flight, f_k , is Gaussian with a mean value of μ_k and a standard deviation, σ_k . As such, we assume we have complete knowledge of the probability density function for each aircraft. Given this density, we can empirically compute the probability that the k^{th} aircraft arrives within the specified interval, $[t_s, t_e]$ by integrating the area under the probability density function within this interval. The Waring's theorem [14] gives the probability that exactly r out of n possible events should occur. Denoting the events A_1, A_2, \dots, A_N the required probability is:

$$\sum_{t=0}^{n-r} (-1)^t \binom{r+t}{t} S_{r+t} \quad (12)$$

where $S_0 = 1$, $S_1 = \sum_i p(A_i)$, and, in general, S_k represents the sum of the probability that any k events occur, regardless of whether the $(n-k)$ events occur. To compute these

probabilities, we implemented an efficient recursive algorithm as presented in a technical report by Radke and Evanoff [15].

As an example, we calculate the distribution of the count of aircraft arriving at SFO in a 15-minute interval (9:45GMT to 10GMT) on July 25th 2012. Figure 2 depicts the distribution of the flight counts, and we can see that the counts distribution is approximately normal. This allows us to use the counts distribution as input to our GBM model, which requires input variables to be normally distributed.

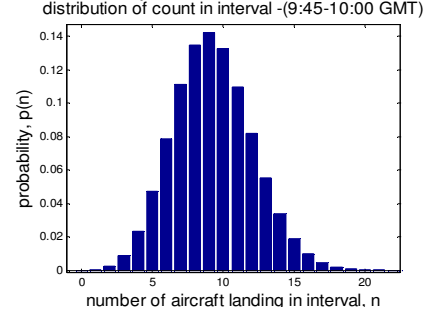


Figure 2. Waring Counts distribution. SFO arrivals 07/25/2012

C. Demand Estimation (PHL)

The demand distribution was obtained using the *ETA to Demands Distribution* methodology described in the previous section with a 15-minute aggregation interval and using TBFM arrivals data. Regarding the uncertainty (σ) associated with the ETAs, we assumed the following values:

- For flights in the air, which have a Scheduled Time of Arrival (STA) assigned by the TBFM system, we assume 1 minute as the standard deviation of delivery time error for the flights to the meter fix. This will only apply to flights outside of the meter fix. We also include an additional terminal standard deviation of 2 minutes. The terminal error reduces linearly with ETA to the runway from 2 minutes at the meter fix to zero error at the runway.
- For flights on the ground, the standard deviation includes the “in the air” standard deviation (i.e. 3 minutes, including meter fix compliance and terminal error) plus 3 minutes of departure compliance error [16].

Note that the σ values above are an educated guess based on previous analysis. A detailed empirical analysis and fine calibration of these parameters is a subject of future research.

D. Prediction Errors

The goal of this section is to evaluate the performance of the GBM model predicting delay and its associated uncertainty. We collected data from 30 snapshots of the TBFM system for PHL (August and October 2014) at about 30 minutes before an arrival push, and we used this data and the GBM model to predict delays up to 90 minutes after the snapshot. The predicted delays are compared with actual arrival times obtained from ASDE-X data.

Figure 3 shows the prediction error for all flights scheduled to arrive up to 90 minutes after one of the snapshots. The prediction error is calculated as the difference between the actual delay and the expected value of the predicted delay

¹ OIS System web. <http://www.fly.faa.gov/ois/>.

distribution. Figure 3 differentiates between flights on the ground, in blue, and in the air, in red. The error for flights in the air is lower than for flight on the ground. The errors (or residuals) need to be distributed around zero, otherwise the GBM model would be consistently over-/under-predicting delays. For flight in the air, the errors are fairly well distributed around zero. On the other hand, the GBM model has a tendency to under-predict delays for flights on the ground.

To better understand the error distribution we generated histograms including flights in the air and on the ground (Figure 4). We can see that the error for flights on the ground is skewed to the right, leading to a mean error of 14.3 minutes. On the other hand, the histogram for flights in the air is symmetric, with a mean error of 2.7 minutes. Flights in the air have an STA assigned by the TBFM system, they are in closed loop, and the chances of flights arriving before or after the assigned STA are comparable, leading to a symmetric distribution. However, the actual arrival time for flights on the ground is more often a later time rather than an earlier time, and this leads to skewness.

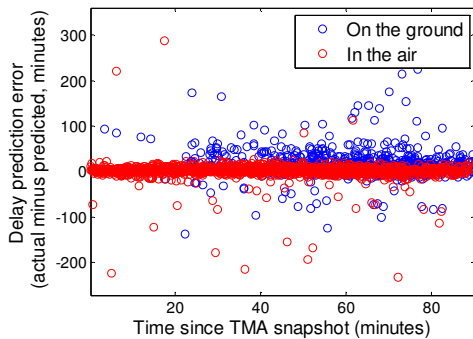


Figure 3. Individual Flight Delay Prediction Error. All Data

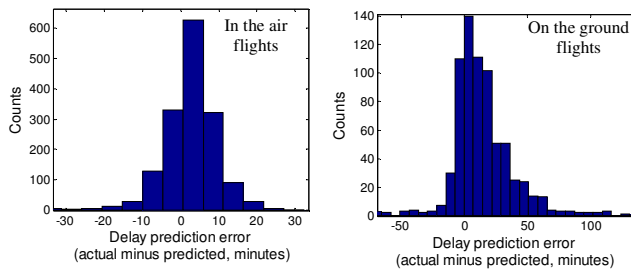


Figure 4. Prediction Error Histograms.

As denoted above, the mean prediction error for flights in the air is 2.7 minutes. This value indicates that our estimate of the capacity may be higher than the actual capacity, leading to delay predictions that are more often under than over the actual delay. If the mean value of the capacity is decreased from 14.5 to 13, the mean error for flights in the air is reduced to 0.17 minutes and for flights on the ground is reduced to 9.7 minutes. The maximum of the histogram for flights on the ground is actually close to 0, but the skewness of the distribution pushes the mean value up to 9.7 minutes. We are modeling capacity with a constant mean and sigma. The

results indicate that the methodology used to estimate PHL capacity may be over-estimating the available capacity. Future research will include a more detailed model of the capacity, where the capacity mean and sigma vary according to the specific conditions at the airport. In addition, predicted delays are lower than actual delays because the GBM model is only estimating delays due to excess demand at the destination. There are other causes of delay not included in the GBM model, for example, delay at the departure airport, airspace congestion, or passenger connectivity. Future research will include additional modeling of out-time prediction error and other effects (e.g., surface congestion, de-icing) to address skewed delay distributions to better model flights on the ground.

Next, we look more in detail at the error of the expected value of the delay distribution predicted by the GBM model. The actual value of the expected delay is not a magnitude we can directly measure. By looking at a flight realized delay we are only looking at a sample of the distribution, and actual delays for successive flights are highly correlated and do not provide a good measure of the actual delay distribution. To obtain an estimate of the actual value of the expected delay, we define buckets for the expected delay provided by the GBM model, and calculate the mean of the actual arrival times for flights which predicted delay falls in each of the buckets. Figure 5 shows the mean of the actual delay for data points with an expected delay value within the defined buckets (x-axis) for two different values of the capacity mean. The size of the buckets was adjusted to make sure that at least 50 flights fell in each bucket. Figure 5 shows that the actual delay increases as the predicted delay increases, and the actuals are over the predicted values, which is consistent with the results presented before for the aggregated histograms. Figure 5 also shows the actual and predicted delay for the reduced capacity we evaluated previously, 13 fl/15 minutes. The lower capacity increases the predicted delay values, leading to actual delay values closer the predicted delays.

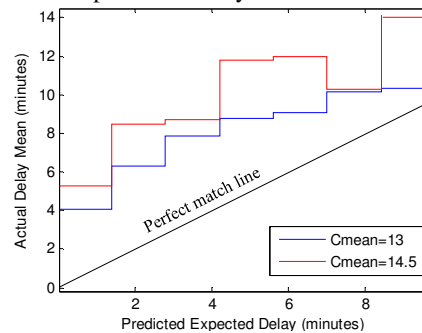


Figure 5. Actual vs Predicted Expected Delay. All flights

We are also interested in evaluating the error of the predicted standard deviation of the delay. As we did for the expected delay we also defined buckets, in this case for the predicted standard deviation. This allow us to identify data points with similar values of the predicted standard deviation. To obtain the actual sigma for each bucket we need the actual mean delay of the distribution for each data point. Because this

value is not directly measurable, we used the expected delay predicted by the GBM model as an estimate. Figure 6 depicts the predicted standard deviation versus the actual standard deviation estimate. For the empirically estimated capacity uncertainty value, 2.5, the actual standard deviation is consistently larger than the predicted deviation. The prediction error can be reduced by increasing the standard deviation of the capacity. Figure 6 shows the error reduction caused by increasing the capacity uncertainty from 2.5 to 3. The GBM model standard deviation does not have a lower limit, and starts at zero; however, as Figure 6 shows, the actual standard deviation is limited at around 3 minutes. Future research will study how to define a lower limit for the standard deviation in the GBM model formulation.

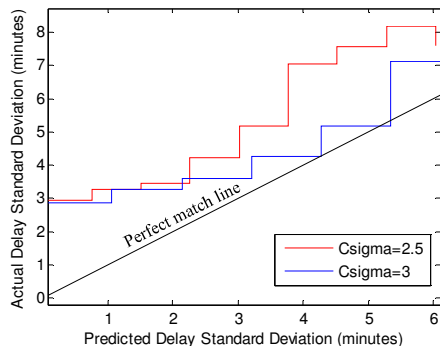


Figure 6. Actual vs Predicted Standard Deviation of the Delay. All flights

IV. CASE STUDIES

In this section we present details for three case studies. The first two case studies show how the GDP and TBFM problems can be modeled using the GBM model. Results for these two case studies are for individual days. The third case study analyzes the interaction between GDP and TBFM metering. This is done by analyzing 30 days of data and comparing the GBM model output (expected delay, over-/under-control probabilities) for the GDP and TBFM metering problem.

A. TBFM Modeling IAH

In this case, we want to consider TBFM metering as the TMI and estimate the probability of under-control and over-control of the TBFM metering program that is being contemplated. The results presented in this analysis are for IAH arrivals.

For our model of TBFM, the demand term in (1) will represent the demand after the application of the STAs at the arrival meter fix. The idea here is to evaluate the TBFM metering program to see if it will work as intended based on the uncertainties in the system. We can also evaluate the TBFM metering program with only the airborne flights to calculate the probability of under-control as a function of time, which will provide an indication of the likelihood that inbound departure flights will be held for a long period of time on the ground before a slot is available due to high delay in the airborne flow.

We took a snapshot of the TMA system 30 minutes before an arrival push, i.e. 15:26 GMT, on May 18th 2014. While

metering was active, the airport was in East configuration with two arrival runways: 08L and 08R. Metering started at around 16:00 GMT and lasted 8 hours.

The demand distribution was obtained using the STAs and ETAs in the TBFM system snapshot and the same methodology and parameters described in Section III.B. We computed the expected capacity based on the expected aircraft mix and the active separation matrix, following the same approach that TBFM uses. At some point in our work, we will add some additional factors to the capacity calculation that TBFM does not use – like dependence with departure demand. But, for our initial work, we computed the expected capacity based on the expected aircraft mix and the active separation matrix. We also applied uncertainty to the capacity. For the capacity uncertainty, we will eventually empirically measure the variance for IAH arrivals. But, in this initial evaluation we assume a standard deviation of 0.5 slots per 10 minute interval. Figure 7 depicts the mean of the demand and capacity for the selected time period.

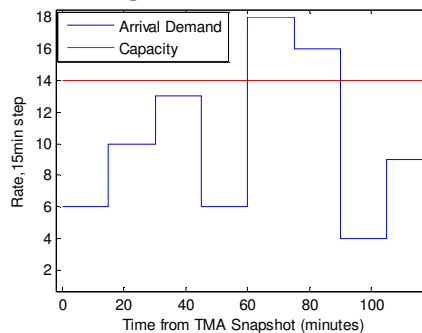


Figure 7. Demand vs Capacity

Figure 8 shows the over-/under-control probabilities for the data in the TMA snapshot and selected parameters. The maximum of the under-control probability for a 5-minute threshold is 0.6. The maximum is reached at the end of the second interval where demand exceeds capacity (Figure 7). The input demand was obtained using the assigned STAs, and ETAs for flights with no STA assigned, which are typically flights on the ground. The results indicate that competing inbound departures would not cause significant issues, since the probability of delay is low even when including inbound departures: the probability of 5 minutes of delay or more is only over 0.5 for 8 minutes (Figure 8).

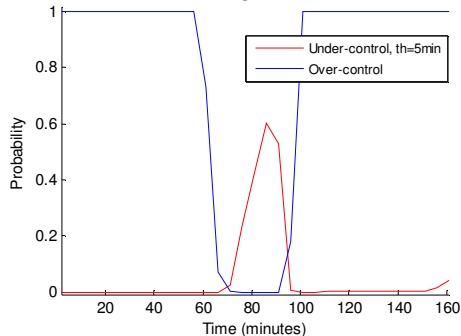


Figure 8. Under-/Over-control probabilities.

B. GDP Modeling – SFO

In this section we address the problem of understanding the nature of the delay distribution which results under the action of a GDP when the time at which the actual capacity will change is uncertain. We specifically study the case where the marine stratus layer at SFO reduces the effective rate of arrivals. Let the capacity of the airport when the weather is clear be denoted by C_{clear} , typically 60 fl/h, and when the runway usage is constrained by the marine stratus as C_{fog} , typically 30 fl/h.

The weather forecast is provided in the form of a probability distribution function that describes the likelihood that the fog will clear at a given time. We refer to the time that the fog clears as t_{clear} . This distribution is provided by the Empirical Cumulative Distribution Function (ECDF) of the difference between the actual and forecast clearing times (errors), for data from 1996 to 2011.

The nominal demand into SFO is assumed to exceed the constrained capacity, C_{fog} , to a degree that some TMI is required to avoid excessive airborne delays. We evaluated two different approaches to model the capacity profile defined by C_{fog} , C_{clear} , and different t_{clear} times and associated probabilities. Both approaches allow us to run the GBM model for the SFO GDP problem and evaluate the over/under-control probabilities.

The necessary demand and GDP parameters were obtained from NAS data for July 25th 2012. The GDP parameters were published at 12:45 GMT. The GDP was scheduled to start at 15:15 GMT and end at 21:14 GMT.

The capacity distribution input to the GBM model needs to be a single curve defined by a set of normally distributed variables, each of them associated with a time interval. The more direct approach to modeling the stratus clearing capacity profile is to have a set of 1-step curves defined by C_{fog} , C_{clear} and t_{clear} and an associated probability linked to t_{clear} . This is the basis of the Pseudo-Monte Carlo (PMC) approach where the GBM model is run for each of the capacity profiles and the over-/under control probabilities are obtained as the weighted sum of the over-/under control probabilities calculated for each capacity profile, and the weights are the probability of occurrence of each profile. The second approach is the analytical approach, in which a single curve captures the uncertainty around the expected clearing time. As an example, Figure 9 shows the capacity profile for July 25th 2012. Both the slope and uncertainty are adjusted using the ECDF of the clearing time prediction errors. The larger the errors the slower the transition from C_{fog} to C_{clear} . The uncertainty increases from its nominal value as we get closer to the clearing forecast time where it reaches its maximum. The PMC methodology was used to validate and calibrate the analytical approach curves, due to space limitation results included in this section are for the analytical approach only.

With respect to the demand distribution, the arrival demand at SFO was generated using ETAs and Control Time of Arrivals (CTAs) available in the NAS data snapshot taken when the GDP parameters were first published. Regarding the

uncertainty associated with the arrival times needed to calculate the demand counts distribution input to the GBM model, we assumed the following σ values:

- For flights in the air we assume a standard deviation of 5 minutes [17].
- For flights on the ground the standard deviation includes the in the air component, 5 minutes, and additionally one of the following departure compliance error values: 15 minutes of departure compliance error [16] for flights with an EDCT assigned, 20 minutes for flights for which an airline CDM message with a predicted runway arrival time was received, 28 minutes for flights for which the departure time was estimated using their PTIME [16].

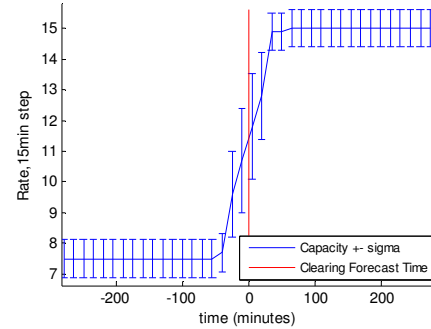


Figure 9. Capacity Profile. Analytical Approach. July 25th 2012

Figure 10 depicts the expected demand counts before the GDP was published, and the capacity profile obtained using the analytical approach. We see that demand exceeds capacity before the fog is expected to clear, and consequently a GDP was necessary to avoid large airborne delays.

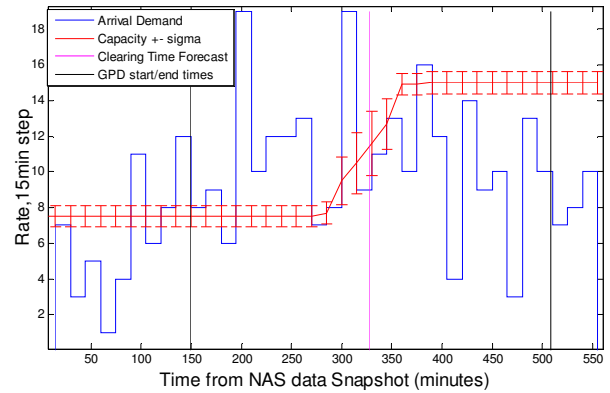


Figure 10. Arrival Demand (before GDP was implemented) vs Capacity.

For the GDP solution (i.e. including controlled times) the maximum expected delay value for July 25th 2012 is 12 minutes. This translates in a probability of under-control reaching only 0.25 for a 15-minute threshold as depicted in Figure 11. The published GDP parameters make delays over 15 minutes unlikely. However, if we reduce the under-control threshold to 5 minutes, as shown in Figure 12 we see that there is a high chance of a 5-minute delay at around 300 minutes. This is 30 minutes before the expected clearing time forecast (shown in magenta in Figure 10).

C. GDP-TBFM Interaction - SFO

In this section we analyze the interaction between two TMIs: GDP and TBFM arrival metering. The goal is to characterize how the implementation of the more strategic TMI (i.e., GDP) affects the down-stream TBFM arrival metering. We do this by comparing the under/over-control probabilities provided by the GBM model for the different initiatives. We look at two

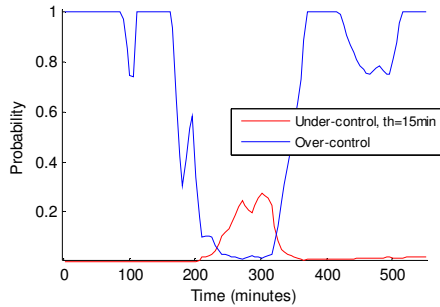


Figure 11. Over-control, Under-control (15-minute threshold) probabilities

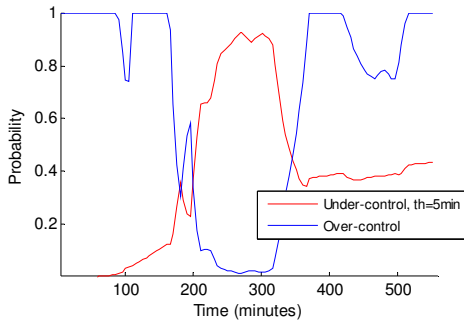


Figure 12. Over-control, Under-control (5-minute threshold) probabilities

different aspects of TBFM. On the one hand, we are interested in comparing the arrival flow constrained by the GDP solution with the arrival capacity seen by the TBFM decision support tool. This comparison will allow us to answer questions like: Is the GDP solution over/under-constraining the arrival flow seen by TBFM metering? On the other hand, we want to evaluate how the Call for Release (CFR) procedure is affected by the GDP solution. In the CFR procedure the Tower must call the Center to coordinate a release time prior to allowing the flight to depart [18]. A GDP solution that did not apply enough ground delay will lead to scarce en route slots, and either large delays for inbound departures ("double delay") or airborne delay.

To obtain meaningful results we processed 30 days of NAS data (2011, 2012 days), and compared the value of the different metrics output of the GBM model over the 30 days.

1) TBFM vs GDP Modeling

The TBFM problem is approximated using the demand in the NAS data. The key difference between GDP modeling as described previously in Section IV.B and TBFM modeling in this case study is the definition of the capacity profile. In the TBFM problem the C_{clear} and C_{fog} values are calculated using the published separation matrices and expected flight mix, and not the rates published in the NAS data. This leads to a more

accurate capacity profile, and will allow us to evaluate the expected delays and over-/under-control probabilities from TBFM's perspective.

2) Results

a) Uncontrolled Case

In the uncontrolled case the arrival demand is generated using ETAs from a NAS data snapshot taken right before the GDP parameters were published. Figure 13 and Figure 14 show the mean and one standard deviation of the under/over-control curves for the 30 days of data (using the forecast clearing time as time reference) for the GDP capacity profile. As expected, these figures show high probability of a 15-minute delay or higher, indicating that the implementation of the GDP was justified. From all the days included, the day with the lowest maximum of the under-control probability was May 27th 2012, with a maximum value of 0.918.

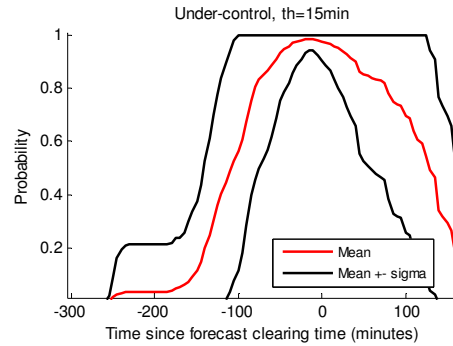


Figure 13. Under-control. Uncontrolled case GDP's view. 30 days of data

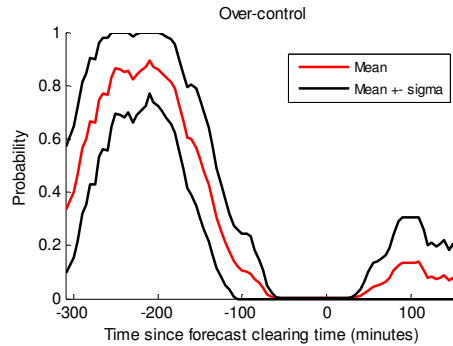


Figure 14. Over-control. Uncontrolled case GDP's view. 30 days of data

These figures can be used to identify when the GDP program should start or end. A good starting time for the GDP program is right before the under-control probabilities spike or the over-control probabilities drop. Figure 13 and Figure 14 denote that somewhere around 200 minutes before the forecast clearing time is typically a good time to start the GDP program.

b) Controlled Case

In the controlled case the arrival demand is generated using ETAs and CTAs available in the NAS data snapshot taken when the GDP parameters are first published.

Under/over-control probabilities for the controlled case and the GDP problem (i.e. using the GDP capacity profile) are

displayed in Figure 15 and Figure 16. The probability of delay reaches its maximum at about 40 minutes before the forecast clearing time. The under-control probability drops before the forecast clearing time. This indicates that capacity increases faster than the arrival rate. Traffic managers are using the clearing forecast time plus a buffer to determine when the arrival flow can be increased to normal levels. The decreasing trend of the under-control probability slows down about 50 minutes after the forecast clearing time, denoting a buffer of about 50 minutes.

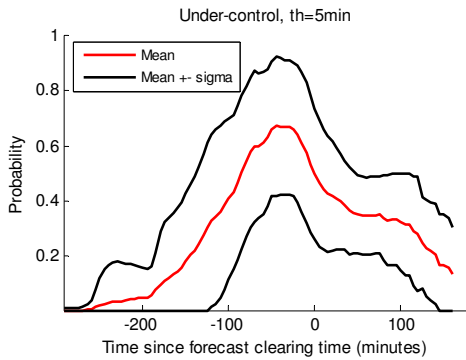


Figure 15. Under-control. Controlled case GDP's view. 30 days of data

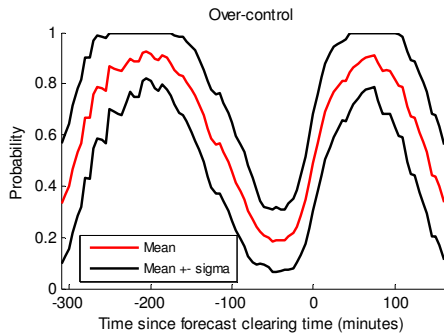


Figure 16. Over-control. Controlled GDP's view. 30 days of data

To study the interaction between GDP and TBFM metering, we run the GBM model for the controlled case using the TBFM capacity profile as described in Section IV.C.1. Figure 17 and Figure 18 depict the under/over-control probabilities. The over-control curve clearly shows that the GDP solution leads to high over-control and most likely to unused capacity. The GDP is typically over-controlling at the TBFM level. The increasing trend in the under-control probability is caused by the increase in uncertainty with time, and the fact that the actual TBFM capacity rate after the fog lifts is typically lower than the rate defined in the NAS data in the GDP context. This is consistent with the published acceptance rates for SFO. For example, for July 25th 2012 the post-fog acceptance rate in the NAS data was 60 fl/h and SFO actual published acceptance rate was 52 fl/h.

A day with especially high delay, and where the GDP solution did not over-control the flow was July 27th 2012. The actual total airborne delay for July 27th was 1617 minutes, which is significantly over the average delay for the 30 days included in this study; the average delay was 373 minutes.

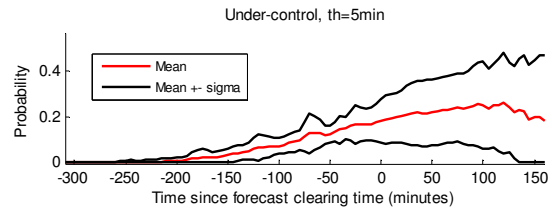


Figure 17. Under-control. Controlled case TBFM's view. 30 days of data

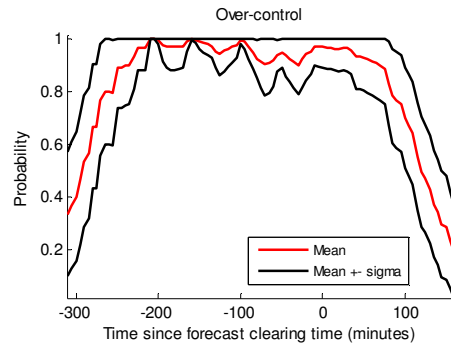


Figure 18. Over-control. Controlled case TBFM's view. 30 days of data

c) Controlled Case – Internal Departures Excluded

In this case, the arrival demand is generated using ETAs and CTAs available in the NAS data snapshot taken when the GDP parameters are first published and excluding internal departures. Internal departures are defined as flights which departure airport is less than 300nm away from SFO. This case is related to the CFR problem, if the probability of under-control is low and the probability of over-control is high, then we would want to recommend that inbound departures find an open slot, rather than competing with airborne flights.

The goal is to evaluate the likelihood of internal departures finding an open slot in the arrival stream in the CFR procedure. On average, the percentage of internal departures for the 30 days included in our study is 21.4%.

Figure 19 and Figure 20 show the under/over-control probabilities for the TBFM capacity profile. The differences between the probabilities including internal departures (Figure 17 and Figure 18), and the probabilities excluding internal departures (Figure 19 and Figure 20) indicate how much additional delay airborne flights would need to accommodate if no control action (additional ground delay) is applied to inbound departures. As these figures show, releasing internal departures does not have a major impact on airborne flights delay, leading to only slightly larger under-control probability, and slightly lower over-control probability.

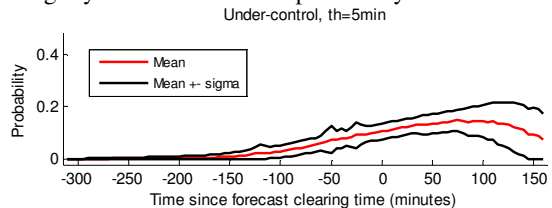


Figure 19. Under-control. Controlled case internal departures excluded, TBFM's view. 30 days of data

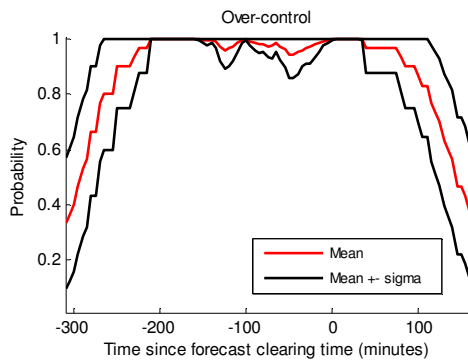


Figure 20. Over-control. Controlled case internal departures excluded, TBFM's view. 30 days of data

V. CONCLUSIONS & NEXT STEPS

The GBM delay prediction model provides an innovative stochastic analytical approach to assess the probability that NAS constraints will over-control or under-control the flow. Case studies demonstrate operational occurrences of over-control that could be addressed using the GBM model. The evaluated case studies include two different TMIs, GDP and TBFM, at SFO, IAH and PHL. The analytical GBM model can be used not only to quickly evaluate a single TMI under uncertainty, but also to study interactions between TMIs by evaluating the likelihood of a TMI (e.g. GDP) over/under-controlling the flow seen by a different TMI (e.g. TBFM metering). Additional work is needed to determine the best approach for integration and display of the GBM model results to operational specialists.

A detailed prediction error analysis was performed on 30 snapshots of the TMA system, including 2,349 flights. The results depicted a mean error of 2.7 minutes in the expected delay for flights in the air, and 14.3 minutes for flights on the ground. These errors were reduced to 0.17 and 9.4 minutes, respectively, by calibrating the arrival capacity. Next steps to improve the GBM model performance include:

- A more detailed characterization of demand and capacity uncertainty parameters: improvements in model accuracy by differentiating among more flight states and uncertainty levels, or detailed capacity modeling, where the capacity μ and σ vary over time according to the state of the capacity constrained resource.
- Additional modeling of out-time prediction error and other effects (e.g., surface congestion, de-icing) to address skewed delay distributions to better model flights on the ground.
- Further development of downstream propagation of demand uncertainty. For example, there could be a sector traveled by some SFO arrivals, which has a chance of being affected by convective weather and its capacity may be reduced. This phenomenon would add additional uncertainty to SFO arrival demand.

VI. ACKNOWLEDGMENTS

This work has been funded under NASA contract NNX14CA55P, however the views expressed herein are solely

those of the authors. The authors thank NASA for the support and guidance received during the performance of this study.

VII. REFERENCES

- [1] J. M. Harrison, *Brownian Motion and Stochastic Flow Systems*, Vol. 121 of Wiley Series in Probability and Statistics, 1985
- [2] S. Grabbe, B. Sridhar, A. Mukherjee, and A. Morando, "Traffic Management Advisor Flow Programs: an Atlanta Case Study," AIAA Guidance, Navigation, and Control Conference, August 2011.
- [3] C. Wanke and C. Taylor, "Exploring Design Trade-offs for Strategic Flow Planning," Aviation Technology, Integration, and Operations Conference, Los Angeles, CA, August 2013.
- [4] T. Nikoleris, M. Hansen, "Queueing Models for Trajectory-Based Aircraft Operations," *Transportation Science*, Vol. 46, No. 4, pp. 501-511, November 2012.
- [5] Roy, S., Sridhar, B., and Verghese, G. C., "An Aggregate Dynamic Stochastic Model for Air Traffic Control," 5th USA/Europe ATM R&D Seminar, Budapest, Hungary, June 2003.
- [6] J. Welch, R. Lloyd, "Estimating airport system delay performance," 4th ATM R&D Seminar, Santa Fe, NM, December 2001.
- [7] Y. Zhou, Y. Wan, S. Roy, C. Taylor, and C. Wanke, "A stochastic modeling and analysis approach to strategic traffic flow management under weather uncertainty," AIAA Guidance, Navigation, and Control Conference, Oregon, August 2011.
- [8] Y. Wan and S. Roy, "A scalable methodology for evaluating and designing coordinated air traffic flow management strategies under uncertainty," *IEEE Transactions on Intelligent Transportation Systems*, vol. 9, no. 4, pp. 644-656, 2008.
- [9] A. Mukherjee, M. Hansen, "Dynamic Stochastic Optimization Model for Air Traffic Flow Management with En Route and Airport Capacity Constraints," 6th USA/Europe ATM R&D Seminar, Baltimore, MD, June 2005.
- [10] R. Hoffman, J. Krozel, G. Davidson, and D. Kierstead, "Probabilistic Scenario-Based Event Planning for Traffic Flow Management," AIAA Guidance, Navigation and Control Conference, 2007.
- [11] C. Pacati, "Brownian Motion and Geometric Brownian Motion" University of Minnesota, academic year 2010-11, unpublished.
- [12] G. Hendeby, F. Gustafsson "On Nonlinear Transformations of Stochastic Variables and its Application to Nonlinear Filtering," ICASSP 2008, Las Vegas, NV, March 2008.
- [13] K. Mueller, R. Bortins, D. Schleicher, D. Sweet, R. Copenbarger, "Effect of uncertainty on en route descent advisor (EDA) predictions," AIAA 4th Aviation Technology, Integration, and Operations Forum, Chicago, 2004.
- [14] A. MacDonald, *Encyclopedia of Actuarial Science*, Publisher John Wiley and Sons, Volume 3, pages 1749-1750, 2004.
- [15] G. Radke, J. Evanoff, "A Fast Recursive Algorithm to Compute the Probability of M-out-of-N Events," Reliability and Maintainability Symposium, Anaheim, CA, 1994.
- [16] A. Capps, S. Engelland, "Characterization of Tactical Departure Scheduling in the National Airspace," 11th AIAA Aviation Technology, Integration, and Operations (ATIO) Conference, Virginia Beach, 2011.
- [17] George Hunter, "ETA Forecasting and Shadow Mode Concepts for the National Airspace," AIAA Aviation 2013, Los Angeles, CA, August 2013.
- [18] S. Engelland, A. Capps, K. Day, M. Kistler, F. Gaither, and G. Juro. "Precision Departure Release Capability (PDRC) Final Report," NASA STI Report, 2013.

VIII. AUTHOR BIOGRAPHY

Juan Rebollo is an Analyst at Mosaic ATM Inc. He received a B.S. in Telecommunications Engineering from the University of Seville and a M.S. in Aeronautics and Astronautics from the Massachusetts Institute of Technology.

Chris Brinton is a Principal Analyst and President at Mosaic ATM Inc. He received a B.S. in Mechanical and Aerospace Engineering from Princeton University and a M.S. in Electrical Engineering from Stanford University.